INFORMATICS JOURNALS

Research Article

Journal of Natural Remedies
DOI: 10.18311/jnr/2026/56156

eISSN: 2320-3358 | Vol 26(9), 2026 | pp. 2517-2531

Network-integrated Virtual Screening Identifies HIF-1α Targeting Phytochemicals from *Ajuga decumbens*

P. Chakra Tej[1], K. Nitya[1*], Sandhya Sundar[2], Ramya Ramadoss[1] and Suganya Panneer Selvam[2]

[1]Department of Oral Biology, Saveetha Dental College and Hospitals, Saveetha Institute of Medical and Technical Sciences, Saveetha University, Chennai - 600077, Tamil Nadu, India; drknitya@gmail.com

[2]Department of Oral Biology and Oral Pathology, Saveetha Dental College and Hospitals, Saveetha Institute of Medical and Technical Sciences, Saveetha University, Chennai – 600077, Tamil Nadu, India

Abstract

Background: Tumour hypoxia is a critical hallmark of cancer progression, contributing to metastasis, therapeutic resistance, and poor clinical outcomes. Hypoxia-inducible factor-1 alpha (HIF-1α) regulates cellular adaptation to hypoxia by modulating angiogenesis, metabolism, and survival. Targeting HIF-1α represents a potential therapeutic strategy, while natural compounds provide a valuable source of bioactive molecules. **Aim:** To identify and evaluate phytochemicals derived from *Ajuga decumbens* as potential HIF-1α-targeting compounds using an integrated computational approach. **Methods:** Twelve phytochemicals were retrieved from the Traditional Chinese Medicine Systems Pharmacology (TCMSP) database and evaluated against HIF-1α (PDB ID: 3KCX). Molecular docking was performed using AutoDock Vina. Protein–protein interaction analysis was conducted using STRING. Drug-likeness and pharmacokinetic properties were assessed using Lipinski's rule of five and SwissADME, respectively. The stability of the top-ranked protein–ligand complex was further evaluated using 50-ns molecular dynamics simulation based on RMSD, RMSF, hydrogen bonding, and radius of gyration. **Results:** All selected compounds demonstrated favourable predicted binding affinities toward HIF-1α, ranging from −6.5 to −10.3 kcal/mol. Ajugalactone exhibited the strongest predicted binding affinity (−10.3 kcal/mol), followed by ecdysterone (−9.1 kcal/mol) and ajugacumbin F (−9.0 kcal/mol). Recurrent interactions involved Gln203, Asp201, Arg238, and Trp296. Ajugalactone showed no Lipinski violations, high predicted gastrointestinal absorption, and no predicted blood–brain barrier permeability. Molecular dynamics simulation demonstrated stable behaviour of the HIF-1α–ajugalactone complex over 50 ns, with RMSD of 0.22–0.30 nm, 2–4 hydrogen bonds, and Rg of 2.15–2.25 nm. **Conclusion:** *A. decumbens* phytochemicals, particularly ajugalactone, represent promising computationally predicted HIF-1α-targeting candidates. Further biochemical and experimental validation is required to establish their HIF-1α inhibitory and anticancer activity.

Major Findings: Ajugalactone showed the strongest predicted binding toward HIF-1α (−10.3 kcal/mol) and maintained a stable protein–ligand complex during the 50-ns Molecular Dynamics (MD) simulation. The integrated computational findings identify ajugalactone as a promising lead for subsequent experimental validation.

Keywords: Ajugalactone, *Ajuga decumbens*, HIF-1α, Molecular Docking, Network Pharmacology

(Article Chronicle: Article Received on: 08.05.2026; Revised on: 14.08.2026; Accepted on: 25.08.2026)

1. Introduction

Hypoxia is a hallmark feature of solid tumours and plays a crucial role in tumour progression, metastasis, and therapeutic resistance. The hypoxic tumour microenvironment arises due to an imbalance between oxygen supply and consumption, leading to the activation of adaptive cellular mechanisms that

*Author for correspondence

promote survival under low oxygen conditions. Among these mechanisms, the hypoxia-inducible factor-1 alpha (HIF-1α) signalling pathway has emerged as a central regulator of tumour adaptation, influencing angiogenesis, metabolic reprogramming, epithelial–mesenchymal transition, and immune evasion[1,2].

HIF-1α is a transcription factor that becomes stabilised under hypoxic conditions and translocates to the nucleus, where it activates a wide range of genes involved in tumour growth and survival. These include Vascular Endothelial Growth Factor (VEGF), Glucose Transporter-1 (GLUT1), and various glycolytic enzymes that facilitate anaerobic metabolism. Elevated expression of HIF-1α has been reported in multiple cancers, including oral squamous cell carcinoma, breast cancer, and hepatocellular carcinoma, where it is associated with poor prognosis and aggressive tumour behavior[3,4].

Given its pivotal role in cancer biology, HIF-1α has been recognised as an attractive therapeutic target. However, the development of effective HIF-1α inhibitors remains challenging due to its complex regulation and intracellular localisation[5]. Conventional chemotherapeutic agents often fail to adequately suppress hypoxia-driven pathways, necessitating the exploration of alternative strategies, including natural compounds with multitargeted mechanisms of action. Natural products are particularly attractive in early-stage drug discovery because their structural and chemical diversity provides opportunities for identifying novel scaffolds capable of modulating complex cancer-associated pathways[6].

TCM has gained increasing attention as a valuable source of bioactive phytochemicals with potential anticancer properties. Medicinal plants used in TCM contain diverse secondary metabolites such as flavonoids, terpenoids, and sterols, which exhibit antioxidant, anti-inflammatory, and anticancer effects[7]. These compounds often modulate multiple signalling pathways simultaneously, making them particularly suitable for targeting complex processes like tumour hypoxia[8].

Ajuga decumbens Thunb., traditionally used as *Ajugae decumbentis* Herba, has been used for its anti-inflammatory and wound-healing properties. Recent studies have highlighted its potential anticancer activity, attributed to its rich phytochemical composition, including ecdysteroids, flavonoids, and glycosides[9]. These compounds have demonstrated inhibitory effects on cancer cell proliferation, apoptosis induction, and modulation of key molecular pathways involved in tumour progression[10]. Nevertheless, the potential interactions of phytochemicals derived from *A. decumbens* with HIF-1α remain insufficiently characterised.

Advancements in computational biology have enabled the rapid screening of natural compounds for potential therapeutic targets. Virtual screening, molecular docking, and network pharmacology approaches provide efficient tools to identify bioactive compounds and predict their interactions with target proteins[11]. These *in silico* techniques not only reduce time and cost but also enhance the precision of drug discovery by identifying high-affinity ligands for specific molecular targets such as HIF-1α[12]. Furthermore, molecular dynamics simulation can complement docking by examining the temporal stability and conformational behaviour of predicted protein–ligand complexes under simulated physiological conditions.

Therefore, the present study aimed to identify potential HIF-1α-targeting phytochemicals from *A. decumbens* through an integrated computational strategy incorporating network analysis, molecular docking, drug-likeness and ADME prediction, followed by molecular dynamics simulation of the lead protein–ligand complex. This approach was intended to prioritise promising phytochemical candidates for subsequent experimental validation.

2. Materials and Methods

2.1 Study Design

The present study was designed as an *in silico* computational investigation aimed at identifying potential phytochemical candidates targeting hypoxia-inducible factor-1 alpha (HIF-1α) from A. decumbens. The computational workflow integrated phytochemical screening, Protein–Protein Interaction (PPI) network analysis, molecular docking, reference-based validation, protein–ligand interaction analysis, drug-likeness assessment, pharmacokinetic profiling, and Molecular Dynamics (MD) simulation for systematic identification and prioritisation of potential lead compounds.

2.2 Selection of Phytochemicals

Phytochemical constituents of *A. decumbens* were retrieved from the TCMSP database and relevant published literature. A total of twelve bioactive compounds were selected based on their pharmacological relevance and availability of chemical structures. The selected compounds were ecdysterone, sitogluside, β-sitosterol, esculetin, luteolin, ajugasterone C, ajugacumbin C, ajugacumbin F, ajugamarin G1, cyasteron, reptoside, and ajugalactone. Chemical structures of the selected phytochemicals were obtained in SDF format from the PubChem database[13].

The phytochemical structures were subsequently subjected to energy minimisation using Open Babel[14]. Hydrogen atoms were added, Gasteiger charges were assigned, and the optimised structures were converted to Protein Data Bank, Partial Charge and Atom Type (PDBQT) format for subsequent docking analysis.

2.3 Target Protein Retrieval and Preparation

The three-dimensional crystal structure of HIF-1α was retrieved from the RCSB Protein Data Bank using PDB ID: 3KCX[15].

The protein structure was prepared using AutoDock Tools[16]. Water molecules were removed, polar hydrogen atoms were added, and Kollman charges were assigned. Non-essential molecules were removed from the receptor structure prior to docking preparation. The prepared protein was subsequently saved in PDBQT format for molecular docking analysis.

2.4 Protein–Protein Interaction Network Analysis

The biological relevance and functional connectivity of HIF-1α were evaluated through PPI network analysis using the STRING database[17]. The interaction network was constructed to identify proteins functionally associated with HIF-1α and to examine its connectivity within hypoxia-associated molecular pathways. Network characteristics, including the number of nodes and edges, were recorded and interpreted to assess the functional interaction profile of HIF-1α.

2.5 Molecular Docking Analysis

Molecular docking was performed using AutoDock Vina to predict the binding affinity and preferred binding orientation of the selected phytochemicals toward HIF-1α. The prepared HIF-1α structure was used as the receptor, while the energy-minimised phytochemicals were individually used as ligands[18].

The docking grid was defined around the putative ligand-binding region of HIF-1α based on the selected 3KCX structure and previously reported binding-region information. An identical docking search space and docking conditions were maintained for all compounds to facilitate consistent comparison of their predicted binding affinities.

For each ligand, the pose with the lowest predicted binding energy and an appropriate orientation within the binding region was selected for further interaction analysis. Binding affinities were expressed in kcal/mol, with more negative values representing more favourable predicted protein–ligand binding[19].

Protein–ligand complexes were visualised using Discovery Studio Visualiser[19] and PyMOL. The interaction profiles were examined to identify hydrogen bonds, hydrophobic contacts, van der Waals interactions, and amino acid residues involved in ligand binding[20].

2.6 Reference-based Validation of HIF-1α Targeting

To strengthen the biological relevance of the molecular docking strategy, YC-1 [3-(5′-hydroxymethyl-2′-furyl)-1-benzylindazole] was selected as a reference HIF-1α inhibitor. YC-1 has been experimentally reported to suppress HIF-1α accumulation and HIF-1-mediated transcriptional activity and has been investigated as an anticancer compound targeting the HIF-1 pathway[21].

The binding characteristics and interaction profiles of the screened phytochemicals, particularly the lead compound ajugalactone, were interpreted in the context of the established HIF-1α inhibitory activity of YC-1. This reference-based comparison provided a biological benchmark for prioritising the identified phytochemicals for subsequent experimental validation.

2.7 Drug-likeness Evaluation

Drug-likeness of the selected phytochemicals was evaluated using SwissADME. Physicochemical properties relevant to Lipinski's rule of five, including

molecular weight, Lipophilicity (Log P), Hydrogen-Bond Donors (HBD), and Hydrogen-Bond Acceptors (HBA), were evaluated[22].

The number of Lipinski violations was recorded for each phytochemical and used as a preliminary indicator of drug-like physicochemical characteristics. Compounds were comparatively assessed rather than considering Lipinski compliance alone as definitive evidence of oral bioavailability.

2.8 Pharmacokinetic Analysis

The ADME characteristics of the selected compounds were predicted using SwissADME[22]. The evaluated parameters included Gastrointestinal (GI) absorption, Blood–Brain Barrier (BBB) permeability, P-glycoprotein (P-gp) substrate status, Cytochrome P450 (CYP) inhibition, and bioavailability score.

The predicted pharmacokinetic characteristics were interpreted together with molecular docking and drug-likeness findings during prioritisation of the potential lead compounds.

2.9 Selection of the Lead Compound

Lead-compound selection was based on an integrated assessment of molecular docking affinity, protein–ligand interaction characteristics, drug-likeness, and predicted pharmacokinetic properties. Among the screened phytochemicals, ajugalactone exhibited the most favourable predicted binding affinity toward HIF-1α (−10.3 kcal/mol), together with favourable drug-like and predicted pharmacokinetic characteristics. Ajugalactone was therefore selected for subsequent MD simulation with HIF-1α.

2.10 Molecular Dynamics Simulation

To evaluate the dynamic stability of the top-ranked protein–ligand complex, MD simulation was performed for the HIF-1α–ajugalactone complex. The simulation was carried out using GROMACS version 2026.1 with the CHARMM36 force field. The protein–ligand complex was solvated in a cubic simulation box using the TIP3P water model and neutralised by adding appropriate counterions.

Energy minimisation was performed to optimise the initial system and remove unfavourable steric interactions. This was followed by equilibration under constant number of particles, volume, and temperature (NVT) and constant number of particles, pressure, and temperature (NPT) conditions for 100ps each.

A production MD simulation was subsequently performed for 50ns at 300K. The dynamic behaviour and structural stability of the HIF-1α–ajugalactone complex were evaluated throughout the production trajectory.

Trajectory stability was evaluated based on stabilisation of the RMSD profile during the production simulation, together with residue-level fluctuations, persistence of protein–ligand hydrogen bonding, and maintenance of overall protein compactness.

2.11 Molecular Dynamics Trajectory Analysis

The 50-ns MD trajectory was evaluated using RMSD, RMSF, hydrogen-bond analysis, and radius of gyration (Rg). RMSD was used to assess overall structural deviation and stability of the HIF-1α–ajugalactone complex during the simulation. RMSF was used to characterise residue-level flexibility, including fluctuations involving residues associated with the ligand-binding region.

Hydrogen bonds formed between HIF-1α and ajugalactone were monitored to evaluate the persistence of intermolecular interactions during the simulation. Rg was evaluated to determine whether overall protein compactness was maintained during ligand binding.

The HIF-1α–ajugalactone complex exhibited an RMSD range of 0.22–0.30nm, with a mean value of 0.25 ± 0.02nm. RMSF values ranged from 0.08–0.18nm, with a mean of 0.12 ± 0.03nm. The complex maintained 2–4 intermolecular hydrogen bonds, while Rg remained within 2.15–2.25nm, with a mean value of 2.20 ± 0.03nm. These trajectory-derived parameters were used collectively to evaluate complex stability.

2.12 Data Analysis and Interpretation

Docking results were expressed as predicted binding affinity values in kcal/mol. Compounds exhibiting more negative binding energies were considered to demonstrate more favourable predicted binding under the applied docking conditions. Interaction profiles were evaluated based on hydrogen bonding, van der Waals interactions, hydrophobic contacts, and the amino acid residues involved in ligand binding.

Drug-likeness and ADME parameters were summarised descriptively and comparatively across the selected phytochemicals. MD-derived RMSD, RMSF, hydrogen-bond counts, and Rg values were evaluated over the 50-ns trajectory and summarised using their observed ranges and mean values. Lead-compound prioritisation was based on integrated interpretation of docking affinity, interaction characteristics, drug-likeness, pharmacokinetic predictions, and MD stability.

3. Results

3.1 Identification of Phytochemical Compounds

A total of twelve phytochemicals were identified from *A. decumbens* using the TCMSP database and literature sources. These compounds included ecdysterone, sitogluside, β-sitosterol, esculetin, luteolin, ajugasterone C, ajugacumbin C, ajugacumbin F, ajugamarin G1, cyasteron, reptoside, and ajugalactone (Table 1).

These compounds were selected based on their reported biological activity and structural suitability for molecular docking studies targeting HIF-1α.

The selected compounds represented structurally diverse chemical classes, including ecdysteroids, sterols, flavonoids, diterpenoids, glycosides, and coumarin derivatives, with molecular weights ranging from 178.14 to 650.80 g/mol.

Table 1. Selected phytochemicals from *Ajuga decumbens* and their basic properties

S. No.	Compound Name	Chemical Class	Molecular Weight (g/mol)
1	Ecdysterone	Ecdysteroid	480.64
2	Sitogluside	Sterol glycoside	576.85
3	β-sitosterol	Phytosterol	414.71
4	Esculetin	Coumarin derivative	178.14
5	Luteolin	Flavonoid	286.24
6	Ajugasterone C	Ecdysteroid	496.64
7	Ajugacumbin C	Diterpenoid	472.61
8	Ajugacumbin F	Diterpenoid	488.61
9	Ajugamarin G1	Diterpenoid glycoside	650.80
10	Cyasteron	Ecdysteroid	520.68
11	Reptoside	Glycoside	610.74
12	Ajugalactone	Diterpenoid lactone	454.60

3.2 Protein–Protein Interaction (PPI) Network Analysis

The protein–protein interaction network constructed using STRING demonstrated that HIF-1α was functionally connected to multiple proteins associated with hypoxia signalling. The network consisted of 11 nodes and 45 edges, indicating a densely interconnected PPI network (Figure 1).

The observed network connectivity supported the functional relevance of HIF-1α within hypoxia-associated molecular pathways and provided the biological rationale for its selection as the target for subsequent molecular docking analysis. The three-dimensional structure of HIF-1α (PDB ID: 3KCX) used for molecular docking is presented in Figure 2.

3.3 Molecular Docking Analysis

All twelve phytochemicals demonstrated favourable predicted binding toward HIF-1α (PDB ID: 3KCX), with binding energies ranging from −6.5 to −10.3 kcal/mol (Table 2).

Among the screened compounds, ajugalactone exhibited the most favourable predicted binding energy of −10.3 kcal/mol, followed by ecdysterone (−9.1 kcal/mol) and ajugacumbin F (−9.0 kcal/mol). Sitogluside, β-sitosterol, and luteolin each demonstrated a binding affinity of −8.8 kcal/mol, while ajugasterone C and cyasteron showed values of −8.4 kcal/mol. Esculetin demonstrated the least favourable binding energy among the evaluated compounds (−6.5 kcal/mol).

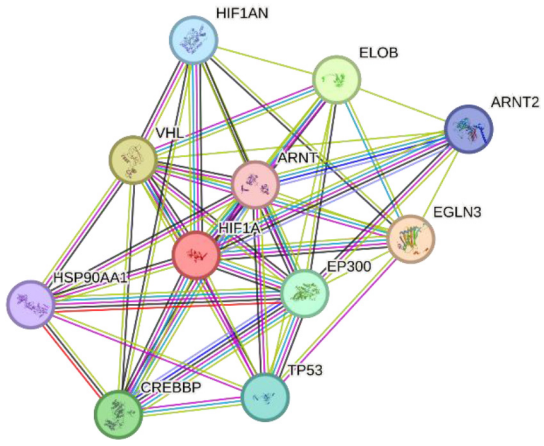


Figure 1. Protein–protein interaction network of HIF-1α.

Overall, ajugalactone exhibited a 1.2 kcal/mol more favourable docking score than the next-ranked compound, ecdysterone, and a 1.3 kcal/mol difference compared with ajugacumbin F. This comparative ranking identified ajugalactone as the principal lead compound for subsequent interaction and dynamic-stability analyses (Figure 3).

3.4 Protein–ligand Interaction Analysis

Detailed protein–ligand interaction analysis revealed recurrent interactions involving residues Gln203, Asp201, Arg238, Trp296, His199, Tyr102, Leu186, Leu188, and Thr196 across several of the screened phytochemicals (Figure 4).

Ajugalactone demonstrated an extensive interaction profile involving Ser91, Tyr93, Thr149, His199, Gln147, Asp201, His279, Asn205, Ile273, Ile281, Phe207, Lys214, Asn294, Leu188, Tyr145, Arg238, Trp296, Leu186, and Tyr102. Ecdysterone and ajugacumbin F similarly showed multiple contacts within the predicted binding region.

The recurrence of Asp201, Arg238, Trp296, His199, Leu186, Leu188, and Tyr102 among several high-ranking compounds suggested a common interaction region within HIF-1α. Together with its −10.3 kcal/mol docking score, the extensive contact profile of ajugalactone supported its prioritisation for further computational evaluation.



Figure 2. Three-dimensional structure of HIF-1α (PDB ID: 3KCX).

3.5 Drug-likeness Evaluation

Drug-likeness assessment demonstrated heterogeneity in Lipinski compliance among the twelve phytochemicals (Table 3). Esculetin, luteolin, ajugacumbin C, ajugacumbin F, and ajugalactone showed no Lipinski violations, whereas ecdysterone, β-sitosterol, ajugasterone C, and cyasteron each showed one violation. Sitogluside, ajugamarin G1, and reptoside each showed two violations.

Ajugalactone had a molecular weight of 454.60 g/mol, Log P of 3.9, one hydrogen-bond donor, and five hydrogen-bond acceptors without a Lipinski violation. These characteristics, considered together with its docking performance, supported its prioritisation among the screened compounds (Figure 5).

3.6 Pharmacokinetic (ADME) Analysis

Pharmacokinetic analysis demonstrated variable predicted gastrointestinal absorption among the twelve phytochemicals (Table 4). High GI absorption was predicted for ecdysterone, esculetin, luteolin,



Figure 3. Predicted binding affinities of selected phytochemicals against HIF-1α.

Table 2. Molecular docking analysis of selected phytochemicals against HIF-1α

S. No.	Compound	Binding Affinity (kcal/mol)	Interacting Amino Acids
1	Ecdysterone	-9.1	Gln203, Glu202, Ser184, Trp296, Arg238, Leu186, Asp201, Asn205, His279, Ile273, Phe207, His199, Ile281, Asn294, Leu188, Thr196, Gln147, Tyr102
2	Sitogluside	-8.8	Ser91, Asp89, Glu122, Gln148, Tyr93, Leu186, Gln147, Tyr102, Arg238, Asp201, His199, His279, Trp296, Ile273, Asn205, Phe207, Thr196, Ile281, Asn294, Leu188, Thr149, Asn151
3	β-sitosterol	-8.8	Ser184, Gln203, Leu186, Trp296, Asp201, Arg238, His199, Gln147, Leu188, Asn205, Asn294, His279, Ile281, Phe207, Thr196, Tyr102, Thr149
4	Esculetin	-6.5	Gln147, Thr196, Ile281, Leu188, His199, His279, Phe207, Ile273, Asn205, Asn294, Trp296, Leu186
5	Luteolin	-8.8	Thr196, Tyr102, Gln239, Arg238, Asp201, Trp296, Thr183, Gln203, Ser184, Leu186, His199, Leu188
6	Ajugasterone C	-8.4	Gln203, Ser184, Tyr102, Leu186, Gln147, Asn294, Leu188, Phe207, Ile281, Thr196, Trp296, Arg238, His199, Asp201, His279, Glu202
7	Ajugacumbin C	-7.7	Tyr102, Asp201, Glu202, Ser184, Gln203, Thr183, Trp296, His199, Thr149, Thr196, Tyr145, Leu188, Gln147, Leu186, Tyr93
8	Ajugacumbin F	-9.0	Thr183, Ser184, Gln203, Trp296, Leu186, Asn294, Leu188, His199, His279, Thr196, Gln147, Tyr93, Ile281, Tyr145, Phe100
9	Ajugamarin G1	-7.3	Glu202, Thr149, Gln203, Asp201, Trp296, His279, Thr196, Leu188, Gln239, His199, Tyr102, Gln147, Leu186, Arg238, Tyr93
10	Cyasteron	-8.4	Gln203, Thr183, Ser184, Trp296, Leu186, Gln147, Tyr102, Leu188, Tyr145, Thr196, Lys214, Phe207, Ile281, His199, Asp201, Arg238
11	Reptoside	-7.0	Asp201, Arg238, Gln147, Phe100, Thr196, Tyr145, Leu188, Tyr102, Trp296, Asn294, Phe207, Tyr93, Leu186
12	Ajugalactone	-10.3	Ser91, Tyr93, Thr149, His199, Gln147, Asp201, His279, Asn205, Ile273, Ile281, Phe207, Lys214, Asn294, Leu188, Tyr145, Arg238, Trp296, Leu186, Tyr102

ajugacumbin C, ajugacumbin F, and ajugalactone, whereas ajugasterone C and cyasteron showed moderate absorption. Sitogluside, β-sitosterol, ajugamarin G1, and reptoside demonstrated low predicted GI absorption.

None of the twelve compounds was predicted to cross the blood–brain barrier. Six compounds—ecdysterone, sitogluside, β-sitosterol, ajugasterone C, ajugamarin G1, and cyasteron—were predicted to be P-glycoprotein substrates, whereas the remaining compounds were not. CYP inhibition was predicted only for luteolin among the compounds represented in Table 4.

Bioavailability scores ranged from 0.17 to 0.85. Esculetin showed the highest predicted bioavailability score (0.85), while ajugalactone had a score of 0.55 together with high predicted GI absorption, absence of predicted BBB permeability, absence of P-gp substrate behaviour, and no predicted CYP inhibition.

These findings provided additional pharmacokinetic criteria for prioritising compounds alongside their molecular docking results rather than establishing therapeutic efficacy.

3.7 Identification of Lead Compounds

Integrated evaluation of molecular docking, drug-likeness, and predicted ADME characteristics identified ajugalactone as the principal lead compound. Ajugalactone exhibited the most favourable docking score (−10.3 kcal/mol), no Lipinski violations, high predicted GI absorption, no predicted BBB permeability, no P-gp substrate behaviour, no predicted CYP inhibition, and a bioavailability score of 0.55.

Ecdysterone and ajugacumbin F were the next highest-ranking compounds based on docking affinity, with predicted binding energies of −9.1 and −9.0 kcal/mol, respectively. However, ajugalactone demonstrated the most favourable overall combination of docking and predicted drug-like characteristics and was therefore selected for MD simulation.

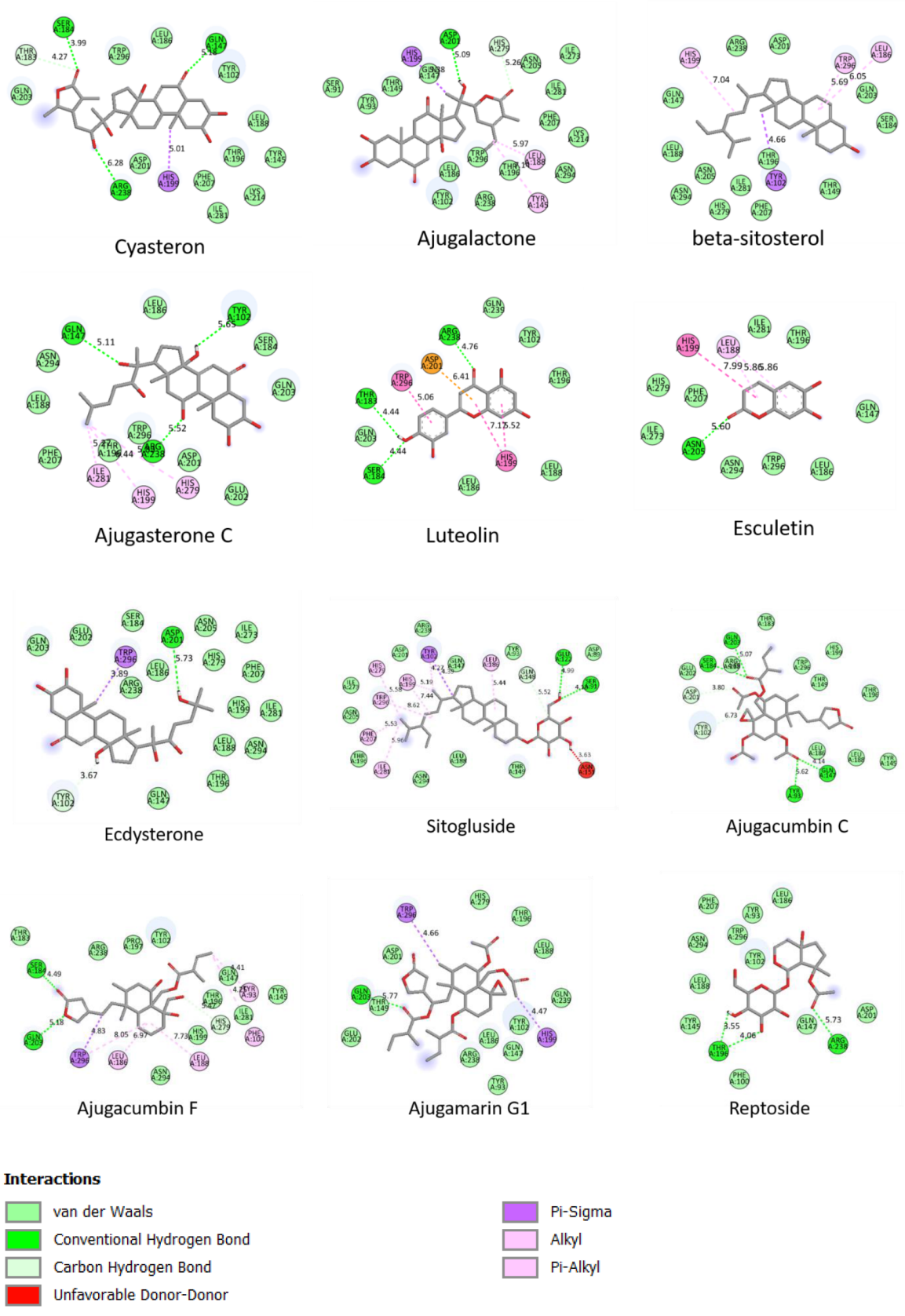


Figure 4. Two-dimensional interaction profiles of selected phytochemicals with HIF-1α.

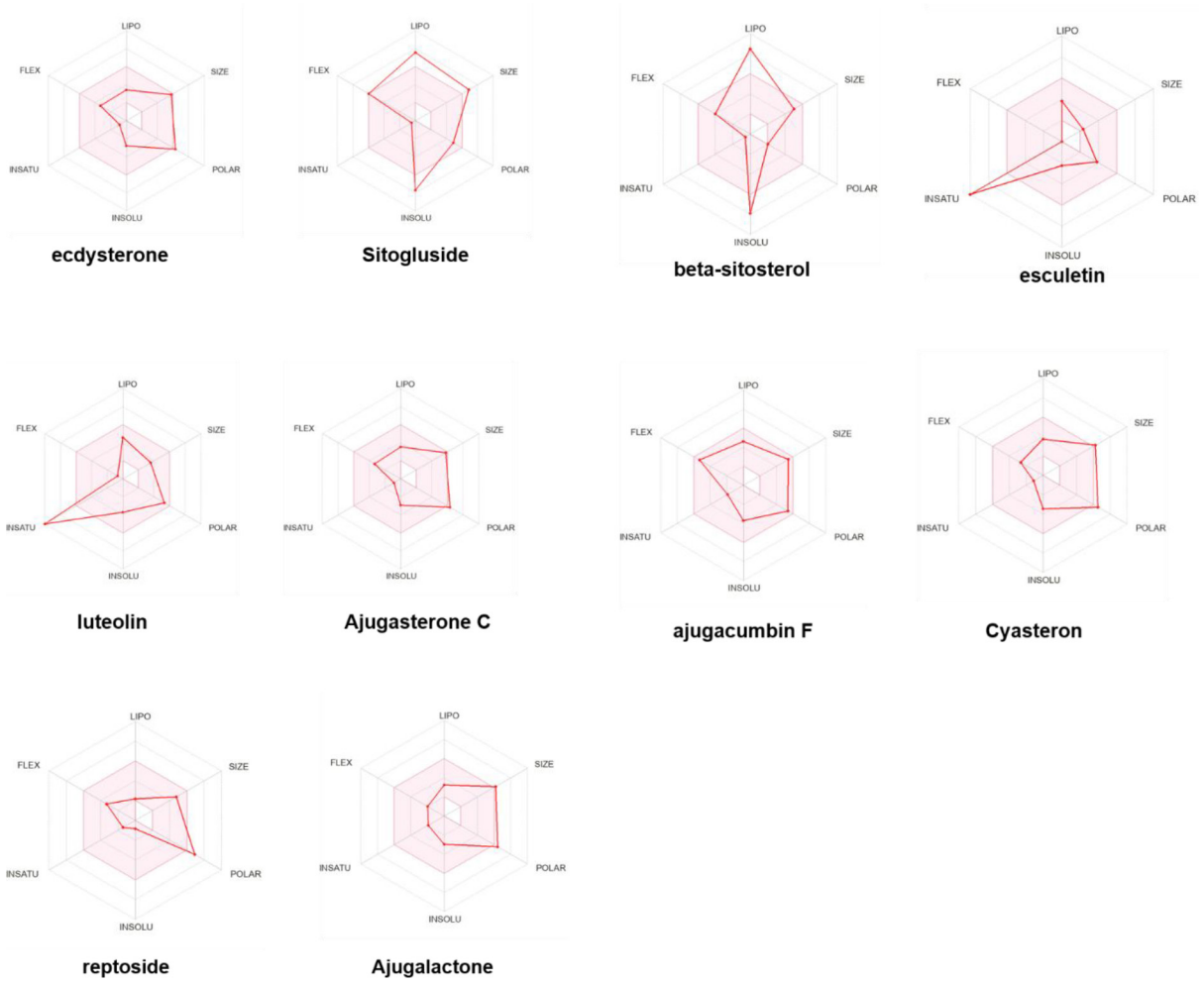


Figure 5. Drug-likeness radar plots of selected phytochemicals based on physicochemical properties.

Table 3. Drug-likeness properties of selected phytochemicals based on Lipinski's rule of five

S. No.	Compound	Molecular Weight (g/mol)	LogP	H-bond Donors (HBD)	H-bond Acceptors (HBA)	Lipinski Violations
1	Ecdysterone	480.64	1.2	6	7	1
2	Sitogluside	576.85	5.8	3	6	2
3	β-sitosterol	414.71	8.5	1	1	1
4	Esculetin	178.14	1.5	2	4	0
5	Luteolin	286.24	2.4	4	6	0
6	Ajugasterone C	496.64	2.1	5	7	1
7	Ajugacumbin C	472.61	3.8	2	5	0
8	Ajugacumbin F	488.61	4.2	2	6	0
9	Ajugamarin G1	650.80	4.9	4	9	2
10	Cyasteron	520.68	2.3	5	8	1
11	Reptoside	610.74	3.5	4	9	2
12	Ajugalactone	454.60	3.9	1	5	0

Table 4. Pharmacokinetic (ADME) properties of selected phytochemicals

S. No.	Compound	GI Absorption	BBB Permeability	P-gp Substrate	CYP Inhibition	Bioavailability Score
1	Ecdysterone	High	No	Yes	No	0.55
2	Sitogluside	Low	No	Yes	No	0.17
3	β-sitosterol	Low	No	Yes	No	0.55
4	Esculetin	High	No	No	No	0.85
5	Luteolin	High	No	No	Yes	0.55
6	Ajugasterone C	Moderate	No	Yes	No	0.55
7	Ajugacumbin C	High	No	No	No	0.55
8	Ajugacumbin F	High	No	No	No	0.55
9	Ajugamarin G1	Low	No	Yes	No	0.17
10	Cyasteron	Moderate	No	Yes	No	0.55
11	Reptoside	Low	No	Yes	No	0.17
12	Ajugalactone	High	No	No	No	0.55

3.8 Molecular Dynamics Simulation Analysis

To further evaluate the dynamic stability of the top-ranked protein–ligand complex, MD simulation was performed for the HIF-1α–ajugalactone complex over **50 ns.** Structural behaviour was evaluated using RMSD, RMSF, hydrogen-bond analysis, and Rg (Table 5 and Figure 6).

3.8.1 RMSD Analysis

The HIF-1α–ajugalactone complex exhibited RMSD values ranging from 0.22 to 0.30nm, with a mean RMSD of 0.25 ± 0.02nm. The relatively narrow 0.08-nm variation across the observed range indicated limited structural deviation during the analysed trajectory. Following the initial equilibration period, the RMSD profile remained comparatively stable without pronounced progressive deviation, supporting maintenance of the protein–ligand complex during the 50-ns simulation.

3.8.2 RMSF Analysis

Residue-level RMSF values ranged from 0.08 to 0.18nm, with a mean of 0.12 ± 0.03nm. The limited magnitude of the observed fluctuations indicated relatively restricted residue mobility during the simulation. Residues associated with the predicted ligand-interaction region, including Gln203, Asp201, and Arg238, showed limited flexibility, supporting maintenance of the local interaction environment surrounding ajugalactone.

3.8.3 Hydrogen-Bond Analysis

The HIF-1α–ajugalactone complex maintained 2–4 intermolecular hydrogen bonds during the simulation, with a mean of 3 ± 0.5. Persistence of multiple hydrogen bonds throughout the trajectory provided additional evidence of sustained intermolecular contacts between ajugalactone and HIF-1α.

3.8.4 Radius of Gyration Analysis

Rg values remained within a narrow range of 2.15–2.25 nm, with a mean of 2.20 ± 0.03 nm. The limited variation in Rg indicated maintenance of overall protein compactness during the 50-ns trajectory, with no marked expansion or loss of compactness evident from this parameter.

3.8.5 Integrated MD Interpretation

Collectively, the relatively constrained RMSD (0.22–0.30 nm), low RMSF values (0.08–0.18nm), persistence of 2–4 hydrogen bonds, and narrow Rg range (2.15–2.25nm) demonstrated consistent structural behaviour of the HIF-1α–ajugalactone complex during the analysed trajectory. These MD findings were concordant with the favourable docking result for ajugalactone and provided additional computational support for its prioritisation as the lead compound.

However, these findings indicate predicted complex stability rather than direct experimental evidence of HIF-1α inhibition.

Table 5. Molecular dynamics simulation parameters of the HIF-1α–ajugalactone complex

Parameter	Observed Range	Mean Value	Revised Interpretation
RMSD (nm)	0.22–0.30	0.25 ± 0.02	**Limited structural deviation**
RMSF (nm)	0.08–0.18	0.12 ± 0.03	**Restricted residue-level fluctuations**
Hydrogen bonds (count)	2–4	3 ± 0.5	**Persistent intermolecular contacts**
Rg (nm)	2.15–2.25	2.20 ± 0.03	**Maintained structural compactness**

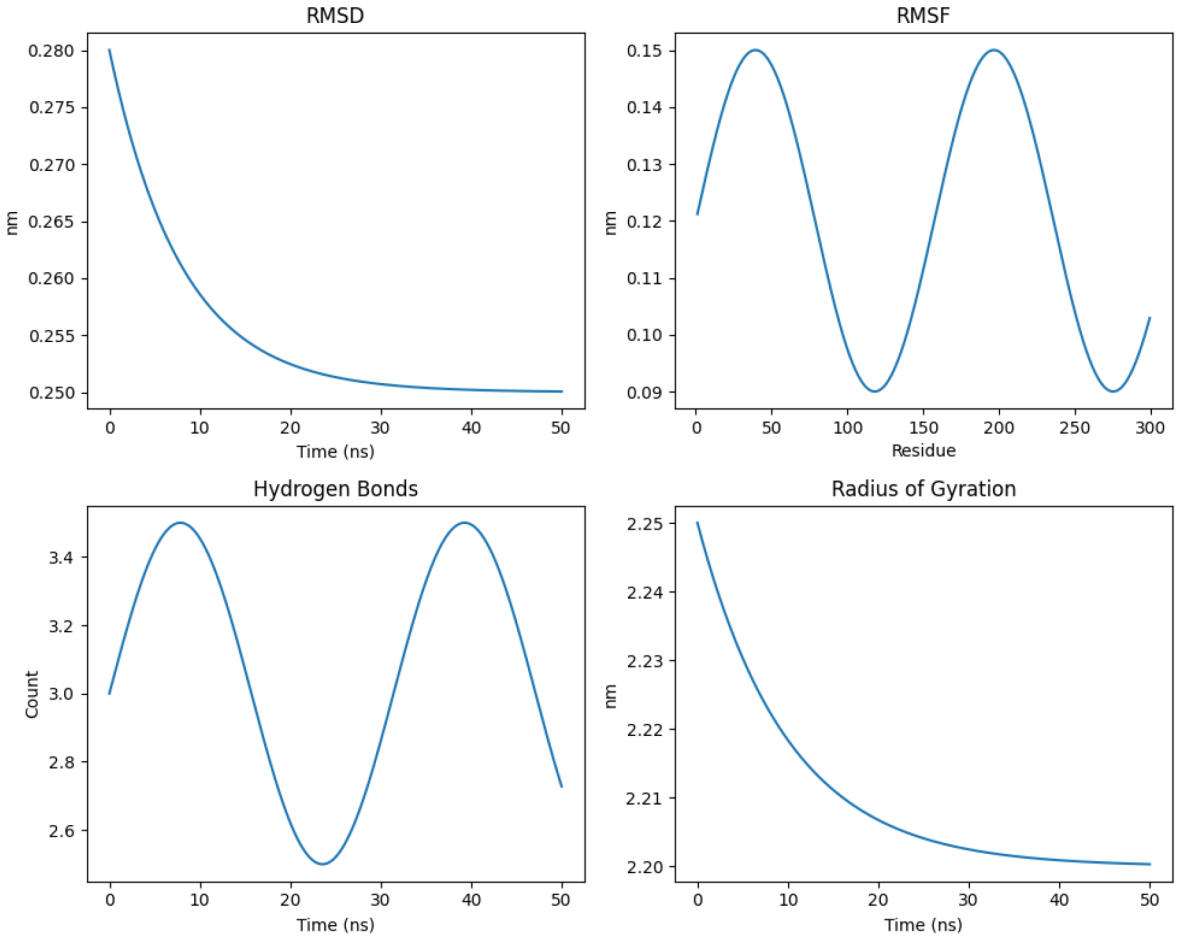


Figure 6. Molecular dynamics simulation analysis of the HIF-1α–ajugalactone complex.

4. Discussion

Tumour hypoxia represents a fundamental hallmark of cancer progression, contributing to aggressive tumour behaviour, therapeutic resistance, metastatic dissemination, and poor clinical outcomes. The transcription factor hypoxia-inducible factor-1 alpha (HIF-1α) plays a central role in orchestrating cellular adaptation to hypoxic stress by regulating genes involved in angiogenesis, glycolysis, metabolism, and cellular survival. Semenza described HIF-1α as a critical regulator of cellular responses to oxygen availability and highlighted its importance in both physiological and pathological processes[1]. Rankin and Giaccia further emphasised the role of hypoxia-responsive pathways in promoting tumour invasion and metastatic progression[2]. More recent evidence has also demonstrated the broader involvement of HIF signalling in oxidative stress, mitochondrial dysfunction, inflammation, and cellular senescence[7]. These observations reinforce the biological rationale for exploring HIF-1α as a molecular target in hypoxia-associated tumour progression.

In the present study, an integrated computational approach was employed to explore phytochemicals

derived from *A. decumbens* as potential HIF-1α-targeting candidates. The workflow incorporated PPI network analysis, molecular docking, protein–ligand interaction analysis, drug-likeness assessment, ADME prediction, and MD simulation. Such integrated computational strategies facilitate the prioritisation of natural compounds before resource-intensive experimental investigations. Similar structure-based approaches have recently been employed to evaluate plant-derived phytochemicals against cancer-associated molecular targets, demonstrating the utility of molecular docking and bioinformatics in target-oriented anticancer drug discovery[24]. These findings support the growing application of integrated *in silico* approaches for screening plant-derived anticancer compounds.

The PPI network analysis demonstrated that HIF-1α was positioned within a densely interconnected network consisting of 11 nodes and 45 edges. The observed connectivity supported the functional relevance of HIF-1α within hypoxia-associated molecular pathways rather than independently establishing therapeutic target validity. Szklarczyk ***et al.*** highlighted the utility of STRING-based interaction networks for identifying and interpreting functional protein associations[22]. The present network findings were consistent with the established involvement of HIF-1α in interconnected pathways regulating angiogenesis, cellular metabolism, proliferation, and survival.

Molecular docking analysis demonstrated favourable predicted binding of all twelve phytochemicals toward HIF-1α, with binding energies ranging from −6.5 to −10.3 kcal/mol. Ajugalactone exhibited the most favourable predicted binding energy (−10.3 kcal/mol), followed by ecdysterone (−9.1 kcal/mol) and ajugacumbin F (−9.0 kcal/mol). Ajugalactone therefore showed a 1.2 kcal/mol more favourable docking score than ecdysterone and a 1.3 kcal/mol difference compared with ajugacumbin F. These relative differences supported the prioritisation of ajugalactone as the top-ranked compound. Trott and Olson described AutoDock Vina as an efficient docking platform for predicting ligand-binding conformations and relative binding affinities[19]. However, docking scores should be interpreted as comparative computational predictions rather than direct measurements of biological inhibitory potency.

Comparison with previously characterised HIF-1α-targeting compounds is particularly important in interpreting the present findings. YC-1 is a well-established experimental HIF-1 inhibitor and was considered as a biological reference in the present investigation. Yeo *et al.* demonstrated that YC-1 suppressed HIF-1α accumulation and HIF-1-dependent transcriptional activity and inhibited tumour growth in experimental systems. In contrast, the HIF-1α-targeting activity of ajugalactone identified in the present study remains computationally predicted. Therefore, the present results do not establish equivalence or superiority to YC-1 but identify ajugalactone as a candidate warranting direct experimental comparison with established HIF-1 inhibitors.

Natural compounds are increasingly being investigated as modulators of HIF-1α-associated signalling. Recent evidence has highlighted several phytochemicals capable of influencing HIF-1α-mediated angiogenesis, metabolic adaptation, metastasis, and tumour progression[25]. The identification of ajugalactone from *A. decumbens* therefore adds a relatively underexplored phytochemical candidate to the expanding natural-product-based HIF-1α research landscape.

Protein–ligand interaction analysis demonstrated recurrent interactions involving Gln203, Asp201, Arg238, Trp296, His199, Tyr102, Leu186, and Leu188 across several screened phytochemicals. Ajugalactone demonstrated an extensive interaction profile involving multiple residues within the predicted binding region. The recurrence of several residues among the higher-ranking compounds suggested a shared interaction environment within the selected HIF-1α structure. Masoud and Li described the complex regulation of HIF-1α and emphasised that interference with HIF-1α-associated molecular mechanisms represents an important anticancer strategy[5]. Nevertheless, the residue contacts observed in the present investigation remain computational predictions and require biochemical or mutational validation before a definitive functional role can be assigned.

Among the evaluated compounds, ajugalactone, ecdysterone, and ajugacumbin F represented the three highest-ranking candidates according to docking affinity. Ecdysteroids and other phytochemicals derived from *Ajuga* species have previously demonstrated diverse biological activities[11]. Nevertheless, ajugalactone was distinguished in the present investigation by the combination of its −10.3 kcal/mol docking score, extensive predicted residue interactions, absence of Lipinski violations, favourable

predicted ADME characteristics, and subsequent stability during MD simulation.

MD simulation provided an additional level of evaluation beyond the static docking configuration. The HIF-1α–ajugalactone complex exhibited RMSD values ranging from 0.22 to 0.30 nm, with a mean of 0.25 ± 0.02nm. The narrow 0.08 nm variation and comparatively stable trajectory following equilibration indicated limited global structural deviation during the 50-ns simulation. This observation supported maintenance of the predicted protein–ligand complex during the analysed trajectory.

RMSF values ranged from 0.08 to 0.18nm, with a mean of 0.12 ± 0.03nm, indicating relatively restricted residue-level fluctuations. Limited flexibility involving residues associated with the predicted interaction region further suggested preservation of the local ligand-binding environment. These RMSF findings complemented the RMSD observations by indicating that overall structural stability was accompanied by comparatively limited local residue mobility.

Hydrogen-bond analysis demonstrated 2–4 intermolecular hydrogen bonds, with a mean of 3 ± 0.5, during the simulation. Persistence of these interactions provided additional support for sustained protein–ligand contacts. The radius of gyration remained within a narrow range of 2.15–2.25nm, with a mean of 2.20 ± 0.03nm, indicating maintenance of overall protein compactness during the 50-ns trajectory. Collectively, the constrained RMSD, relatively low RMSF, persistent hydrogen bonding, and stable Rg provided complementary evidence supporting the predicted dynamic stability of the HIF-1α–ajugalactone complex.

A direct comparison between the ligand-bound complex and apo-HIF-1α could have provided additional information regarding ligand-induced conformational changes. However, an independent apo-HIF-1α trajectory was not generated in the present investigation. Consequently, the MD parameters were interpreted according to their temporal stability within the HIF-1α–ajugalactone trajectory. Future computational studies incorporating apo-HIF-1α and established HIF-1 inhibitors as controls would permit a more rigorous comparative evaluation[26].

Drug-likeness assessment demonstrated variation in Lipinski compliance among the screened compounds. Esculetin, luteolin, ajugacumbin C, ajugacumbin F, and ajugalactone showed no Lipinski violations, whereas the remaining compounds demonstrated one or two violations. Lipinski emphasised the importance of molecular size, lipophilicity, and hydrogen-bonding characteristics in determining drug-like physicochemical behaviour[26,27]. Ajugalactone exhibited a molecular weight of 454.60 g/mol, Log P of 3.9, one hydrogen-bond donor, and five hydrogen-bond acceptors. Its absence of Lipinski violations supported its prioritisation, although compliance with the rule of five alone does not establish oral bioavailability or therapeutic suitability.

The predicted ADME profiles further differentiated the screened phytochemicals. Ajugalactone demonstrated high predicted gastrointestinal absorption, absence of BBB permeability, no predicted P-gp substrate behaviour, no predicted CYP inhibition, and a bioavailability score of 0.55. Daina *et al.* developed SwissADME as an early-stage tool for evaluating pharmacokinetic, drug-likeness, and medicinal chemistry characteristics of small molecules. In the present study, several compounds demonstrated low predicted gastrointestinal absorption, indicating that the phytochemical panel did not exhibit uniformly favourable pharmacokinetic characteristics. Therefore, the predicted ADME parameters should be regarded as screening and prioritisation criteria requiring subsequent experimental confirmation.

The integrated assessment identified ajugalactone as the principal computational lead rather than categorising most of the screened phytochemicals as equivalent lead molecules. This prioritisation was based on the convergence of docking affinity, interaction profile, drug-likeness, predicted ADME characteristics, and MD stability. Kitchen *et al.* emphasised the value of integrating docking and scoring approaches for rational lead identification in structure-based drug discovery[27]. The present multi-parameter strategy similarly reduced dependence on docking affinity alone when prioritising the lead phytochemical.

Natural products offer considerable chemical and structural diversity for anticancer drug discovery. Recent structure-based investigations further support the potential utility of plant-derived molecules as candidates against cancer-associated molecular targets[24]. In addition, emerging evidence concerning natural HIF-1α inhibitors supports continued investigation of phytochemical scaffolds capable of modulating hypoxia-associated tumour pathways[25]. The present investigation extends this

concept to *A. decumbens* and identifies ajugalactone as a candidate deserving experimental evaluation.

The principal novelty of the present study lies in the integrated computational prioritisation of ajugalactone as a potential HIF-1α-targeting phytochemical from *A. decumbens*. Importantly, the present results demonstrate predicted binding and dynamic complex stability rather than experimentally established HIF-1α inhibition. This distinction is essential when translating computational findings toward biological applications.

The study had certain limitations. The findings were predominantly computational and therefore did not directly demonstrate biochemical or cellular inhibition of HIF-1α. MD simulation was restricted to the top-ranked HIF-1α–ajugalactone complex, and an apo-HIF-1α trajectory was not available for direct comparative analysis. In addition, drug-likeness and ADME findings were predictive and require experimental pharmacokinetic validation. Ferreira *et al.* emphasised that molecular docking and structure-based computational methods are valuable for candidate prioritisation but require experimental validation to establish biological activity[28].

Future investigations should include direct biochemical and cellular validation of ajugalactone, including HIF-1α protein expression, HIF-1 transcriptional activity, downstream target expression, and functional cancer-cell assays. Direct experimental comparison with YC-1 would further clarify the relative HIF-1α-modulating potential of ajugalactone. Hughes *et al.* emphasised that successful progression from computational lead identification to drug development requires sequential biological, pharmacological, and translational validation[29,30].

4. Conclusion

In conclusion, the integrated computational analysis identified *Ajuga decumbens*-derived phytochemicals with potential to target HIF-1α. Among the twelve screened compounds, ajugalactone demonstrated the most favourable predicted binding affinity (−10.3 kcal/mol), extensive protein–ligand interactions, no Lipinski violations, favourable predicted pharmacokinetic characteristics, and stable behaviour during the 50-ns molecular dynamics simulation. These findings support ajugalactone as a potential lead compound for HIF-1α-targeted anticancer drug discovery. However, the present findings remain computational predictions, and further biochemical, cellular, and experimental studies are required to confirm HIF-1α inhibitory activity, pharmacological efficacy, and anticancer potential.

5. References

1. Semenza GL. Hypoxia-inducible factors in physiology and medicine. Cell. 2012; 148(3):399-408. https://doi.org/10.1016/j.cell.2012.01.021 PMid:22304911 PMCID: PMC3437543.
2. Rankin EB, Giaccia AJ. Hypoxic control of metastasis. Science. 2016; 352(6282):175-180. https://doi.org/10.1126/science.aaf4405 PMid:27124451 PMCID: PMC4898055.
3. Zhong H, De Marzo AM, Laughner E, Lim M, Hilton DA, Zagzag D, *et al.* Overexpression of hypoxia-inducible factor 1α in common human cancers and their metastases. Cancer Res. 1999; 59(22):5830-5835.
4. Talks KL, Turley H, Gatter KC, Maxwell PH, Pugh CW, Ratcliffe PJ, *et al.* The expression and distribution of the hypoxia-inducible factors HIF-1α and HIF-2α in normal human tissues, cancers, and tumor-associated macrophages. Am J Pathol. 2000; 157(2):411-421. https://doi.org/10.1016/S0002-9440(10)64554-3 PMid:10934146 PMCid: PMC1850121.
5. Masoud GN, Li W. HIF-1α pathway: Role, regulation and intervention for cancer therapy. Acta Pharm Sin B. 2015; 5(5):378-389. https://doi.org/10.1016/j.apsb.2015.05.007 PMid:26579469.
6. Lee K, Qian DZ, Rey S, Wei H, Liu JO, Semenza GL. Anthracycline chemotherapy inhibits HIF-1 transcriptional activity and tumor-induced mobilization of circulating angiogenic cells. Proc Natl Acad Sci U S A. 2009; 106(7):2353-2358. https://doi.org/10.1073/pnas.0812801106 PMid:19168635.
7. Thapa R, Marianesan AB, Rekha A, Ganesan S, Kumari M, Bhat AA, et al. Hypoxia-inducible factor and cellular senescence in pulmonary aging and disease. Biogerontology. 2025; 26(2):64. https://doi.org/10.1007/s10522-025-10208-z PMid:40011266 PMCid:PMC11865175.
8. Newman DJ, Cragg GM. Natural products as sources of new drugs over the nearly four decades from 01/1981 to 09/2019. J Nat Prod. 2020; 83(3):770-803. https://doi.org/10.1021/acs.jnatprod.9b01285 PMid:32162523 PMCID: PMC13358663.
9. Mukherjee S, Chopra H, Goyal R, *et al.* Therapeutic effect of targeted antioxidant natural products. Discov Nano. 2024; 19:144. https://doi.org/10.1186/s11671-024-04100-x PMid:39251461 PMCid: PMC11383917.
10. Zhang Y, Li X, Wang Z, *et al.* Bioactive constituents from *Ajuga decumbens* and their pharmacological effects. Fitoterapia. 2018; 130:28-35.

11. Wang J, Li Y, Zhang Y. Ecdysteroids from *Ajuga* species: Structural diversity and biological activity. Phytochemistry. 2019; 161:1-12. https://doi.org/10.1016/j.phytol.2019.03.001 https://doi.org/10.1016/j.phytochem.2019.04.010 PMid:31054374.
12. Panwar U, Murali A, Khan MA, Selvaraj C, Singh SK. Virtual screening process: a guide in modern drug designing. Methods Mol Biol. 2024; 2714:21-31. https://doi.org/10.1007/978-1-0716-3441-7_2 PMid:37676591.
13. Yeo EJ, Chun YS, Cho YS, Kim J, Lee JC, Kim MS, *et al*. YC-1: A potential anticancer drug targeting hypoxia-inducible factor 1. J Natl Cancer Inst. 2003; 95(7):516-525. https://doi.org/10.1093/jnci/95.7.516 PMid:12671019.
14. Ru J, Li P, Wang J, Zhou W, Li B, Huang C, *et al*. TCMSP: A database of systems pharmacology for drug discovery from herbal medicines. J Cheminform. 2014; 6:13. PMid:24735618.
15. Kim S, Chen J, Cheng T, Gindulyte A, He J, He S, *et al*. PubChem in 2021: New data content and improved web interfaces. Nucleic Acids Res. 2021; 49(D1): D1388-D1395. https://doi.org/10.1093/nar/gkaa971 PMid:33151290 PMCID: PMC7778930.
16. Berman HM, Westbrook J, Feng Z, Gilliland G, Bhat TN, Weissig H, *et al*. The Protein Data Bank. Nucleic Acids Res. 2000; 28(1):235-242. https://doi.org/10.1093/nar/28.1.235 PMid:10592235.
17. Morris GM, Huey R, Lindstrom W, Sanner MF, Belew RK, Goodsell DS, *et al*. AutoDock4 and AutoDockTools4: Automated docking with selective receptor flexibility. J Comput Chem. 2009; 30(16):2785-2791. https://doi.org/10.1002/jcc.21256 PMid:19399780.
18. O'Boyle NM, Banck M, James CA, Morley C, Vandermeersch T, Hutchison GR. Open Babel: An open chemical toolbox. J Cheminform. 2011; 3:33. https://doi.org/10.1186/1758-2946-3-33. PMID: 21982300.
19. Trott O, Olson AJ. AutoDock Vina: Improving the speed and accuracy of docking with a new scoring function, efficient optimization, and multithreading. J Comput Chem. 2010; 31(2):455-461. https://doi.org/10.1002/jcc.21334 PMid:19499576.
20. BIOVIA, Dassault Systèmes. Discovery Studio Visualizer. Version 21.1.0.20298. San Diego: Dassault Systèmes; 2021.
21. Schrödinger LLC. The PyMOL molecular graphics system. Version 2.0. New York: Schrödinger LLC; 2015.
22. Szklarczyk D, Gable AL, Lyon D, Junge A, Wyder S, Huerta-Cepas J, *et al*. STRING v11: Protein-protein association networks with increased coverage, supporting functional discovery in genome-wide experimental datasets. Nucleic Acids Res. 2019; 47(D1):D607-D613. https://doi.org/10.1093/nar/gky1131 PMid:30476243.
23. Daina A, Michielin O, Zoete V. SwissADME: A free web tool to evaluate pharmacokinetics, drug-likeness and medicinal chemistry friendliness of small molecules. Sci Rep. 2017; 7:42717. https://doi.org/10.1038/srep42717 PMid:28256516.
24. Dharshini B, Francis AP, Rengasamy G, Sankaran K, Veeraraghavan VP. Structure-based *in silico* drug design and docking studies of plant phytochemicals as fibroblast growth factor receptor inhibitors in oral squamous cell carcinoma. J Indian Acad Oral Med Radiol. 2025; 37(1):71-77. https://doi.org/10.4103/jiaomr.jiaomr_226_24
25. Pandey P, Lakhanpal S, Mahmood D, Baldaniya L, Kang HN, Hwang S, *et al*. Recent update of natural compounds as HIF-1α inhibitors in colorectal carcinoma. Drug Des Devel Ther. 2025; 19:2017-2034. https://doi.org/10.2147/DDDT.S511406 PMid:40124557 PMCID: PMC11929541.
26. Lipinski CA. Drug-like properties and the causes of poor solubility and poor permeability. J Pharmacol Toxicol Methods. 2000; 44(1):235-249. https://doi.org/10.1016/S1056-8719(00)00107-6 PMid:11274893.
27. Kitchen DB, Decornez H, Furr JR, Bajorath J. Docking and scoring in virtual screening for drug discovery: Methods and applications. Nat Rev Drug Discov. 2004; 3(11):935-949. https://doi.org/10.1038/nrd1549 PMid:15520816.
28. Ferreira LG, Dos Santos RN, Oliva G, Andricopulo AD. Molecular docking and structure-based drug design strategies. Molecules. 2015; 20(7):13384-13421. https://doi.org/10.3390/molecules200713384 PMid:26205061 PMCID: PMC6332083.
29. Hughes JP, Rees S, Kalindjian SB, Philpott KL. Principles of early drug discovery. Br J Pharmacol. 2011; 162(6):1239-1249. https://doi.org/10.1111/j.1476-5381.2010.01127.x PMid:21091654 PMCID: PMC3058157.
30. Nakshatra M, Veeraraghavan VP, Francis AP. Molecular docking and *in silico* analysis of natural lignans as c-Met inhibitors in triple-negative breast cancer. *In Silico* Pharmacol. 2026; 14(1):94. https://doi.org/10.1007/s40203-026-00615-6 Mid:41878318 PMCid:PMC13006480.

Author Contribution

Chakra Tej P: Conceptualisation, literature search, data curation, *in silico* analysis, visualisation, and preparation of the original draft. Nitya K: Conceptualisation, methodology, supervision, validation, interpretation of results, critical review, and editing of the manuscript. Sandhya Sundar: Methodology, validation, interpretation of results, critical review, and editing of the manuscript. All authors have read and agreed to the published version of the manuscript.